

Articles

Synthesis and Characterizations of Cyclometalated Iridium(III) Solvento Complexes

B. Schmid, F. O. Garces, and R. J. Watts*

Department of Chemistry, University of California, Santa Barbara, California 93106

Received July 2, 1993*

Complexes of the type $[\text{Ir}(\text{L})_2(\text{S})_2][\text{OTf}]$ have been prepared by reactions of $[\text{Ir}(\text{L})_2\text{Cl}]_2$ with AgOTf in an appropriate solvent medium ($\text{L} = 2\text{-phenylpyridine (ppy) or } 2\text{-}(p\text{-tolyl)pyridine (ptpy)}$; $\text{S} = \text{H}_2\text{O or CH}_3\text{CN}$; $\text{OTf} = \text{CF}_3\text{SO}_3^-$). These solvento complexes have been characterized by ^1H and ^{13}C NMR spectroscopies, UV-visible absorption and emission spectroscopies, and cyclic voltammetry. Estimates of radiative lifetimes based upon weak integrated absorption bands in the 460–490-nm region are in agreement with emission lifetimes monitored in glasses at 77 K. Low-lying excited states responsible for these absorption and emission bands are assigned to an admixture of ligand-localized and metal-to-ligand charge-transfer character. Quenching of the emissions in ambient solutions is discussed in terms of ligand labilization due to either thermal population of metal-centered excited states or direct labilization in the MLCT excited state due to enhanced *trans* effects of the Ir–C bonds on the Ir–S bonding.

Introduction

The 2-phenylpyridine ligand (Hppy) reacts with a variety of transition metal centers to yield cyclometalated products.^{1–5} Photophysical and photochemical studies of cyclometalated Ir(III) complexes of ppy and related ligands^{6–14} indicate that they are strong photoreducing agents as a result of a combination of their high-energy emissive excited states and the ease with which the metal center is oxidized. Facile oxidation of the metal center also leads to long-lived metal-to-ligand charge-transfer (MLCT) excited states in many instances,^{15–39} and these are well suited to operate as sensitizers for outer-sphere electron-transfer

reactions.^{40–43} These strongly photoreductive MLCT excited states may be useful sensitizers for CO_2 reduction.^{44–54}

Cyclometalated Ir(III) complexes which contain weakly bound solvent ligands might be useful catalyst precursors in homogeneous

* Abstract published in *Advance ACS Abstracts*, December 1, 1993.

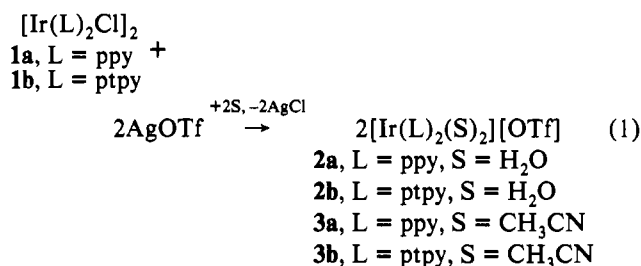
- (1) Dehand, J.; Pfeffer, M. *Coord. Chem. Rev.* **1976**, *18*, 327.
- (2) Bruce, M. I. *Angew. Chem., Int. Ed. Engl.* **1977**, *16*, 73.
- (3) Omae, I. *Chem. Rev.* **1979**, *79*, 287.
- (4) Omae, I. *Coord. Chem. Rev.* **1980**, *32*, 235.
- (5) Parshall, G. W. *Acc. Chem. Res.* **1970**, *3*, 139.
- (6) Ohsawa, Y.; Sprouse, S.; King, K. A.; DeArmond, M. K.; Hanck, K. W.; Watts, R. J. *J. Phys. Chem.* **1987**, *91*, 1047.
- (7) Sprouse, S.; King, K. A.; Spellane, P. J.; Watts, R. J. *J. Am. Chem. Soc.* **1984**, *106*, 6647.
- (8) King, K. A.; Garces, F. O.; Sprouse, S.; Watts, R. J. *Proceedings of the 7th International Symposium on the Photochemistry and Photophysics of Coordination Compounds*; Yersin, H., Vogler, A., Eds.; Springer Verlag: Berlin, **1987**; p 141.
- (9) Ichimura, K.; Kobayashi, T.; King, K. A.; Watts, R. J. *J. Phys. Chem.* **1987**, *91*, 6104.
- (10) Garces, F. O.; King, K. A.; Watts, R. J. *Inorg. Chem.* **1988**, *27*, 3464.
- (11) Garces, F. O.; Watts, R. J. *Inorg. Chem.* **1990**, *29*, 582.
- (12) King, K. A.; Watts, R. J. *J. Am. Chem. Soc.* **1987**, *109*, 1589.
- (13) King, K. A.; Spellane, P. J.; Watts, R. J. *J. Am. Chem. Soc.* **1985**, *107*, 1431.
- (14) King, K. A.; Finlayson, M. F.; Spellane, P. J.; Watts, R. J. *Sci. Pap. Inst. Phys. Chem. Res. (Jpn.)* **1984**, *78*, 97.
- (15) Sandrini, D.; Maestri, M.; Balzani, V.; Chassot, L.; von Zelewsky, A. *J. Am. Chem. Soc.* **1987**, *109*, 7720.
- (16) Maestri, M.; Sandrini, D.; Balzani, V.; Chassot, L.; Jolliet, P.; von Zelewsky, A. *Chem. Phys. Lett.* **1985**, *122*, 375.
- (17) Chassot, L.; von Zelewsky, A.; Sandrini, D.; Maestri, M.; Balzani, V. *J. Am. Chem. Soc.* **1986**, *108*, 6084.
- (18) Schwarz, R.; Gliemann, G.; Jolliet, P.; von Zelewsky, A. *Inorg. Chem.* **1989**, *28*, 1053.
- (19) Craig, C. A.; Garces, F. O.; Watts, R. J.; Palmans, R.; Frank, A. J. *Coord. Chem. Rev.* **1990**, *97*, 193.
- (20) Bar, L.; Gliemann, G.; Chassot, L.; von Zelewsky, A. *Chem. Phys. Lett.* **1986**, *123*, 264.
- (21) Chassot, L.; von Zelewsky, A. *Inorg. Chem.* **1987**, *26*, 2814.
- (22) Bonafede, S.; Ciano, M.; Bolletta, F.; Balzani, V.; Chassot, L.; von Zelewsky, A. *J. Phys. Chem.* **1986**, *90*, 3836.
- (23) Sandrini, D.; Maestri, M.; Ciano, M.; Balzani, V.; Lüönd, R.; Deuschel-Cornioley, C.; Chassot, L.; von Zelewsky, A. *Gazz. Chim. Ital.* **1988**, *118*, 661.
- (24) Schwarz, R.; Gliemann, G.; Chassot, L.; Jolliet, P.; von Zelewsky, A. *Helv. Chim. Acta* **1989**, *72*, 1.
- (25) Cornioley-Deuschel, C.; von Zelewsky, A. *Inorg. Chem.* **1987**, *26*, 3354.
- (26) Barigelletti, F.; Sandrini, D.; Maestri, M.; Balzani, V.; von Zelewsky, A.; Chassot, L.; Jolliet, P.; Mäder, U. *Inorg. Chem.* **1988**, *27*, 3644.
- (27) Balzani, V.; Maestri, M.; Melandri, A.; Sandrini, D.; Chassot, L.; Cornioley-Deuschel, C.; Jolliet, P.; Mäder, U.; von Zelewsky, A. *Photochemistry and Photophysics of Coordination Compounds*; Yersin, H.; Vogler, A., Eds.; Springer Verlag: Berlin **1987**; p 71.
- (28) Lees, A. J. *Chem. Rev.* **1987**, *87*, 711.
- (29) Reveco, P.; Schmehl, H.; Cherry, W. R.; Fronczek, F. R.; Selbin, J. *Inorg. Chem.* **1985**, *24*, 4078.
- (30) Reveco, P.; Cherry, W. R.; Medley, J.; Garber, A.; Gale, R. J.; Selbin, J. *Inorg. Chem.* **1986**, *25*, 1842.
- (31) Wakatsuki, Y.; Yamazaki, H.; Grutsch, P. A.; Santhanam, M.; Katal, C. *J. Am. Chem. Soc.* **1985**, *107*, 8153.
- (32) Craig, C. A.; Watts, R. J. *Inorg. Chem.* **1989**, *28*, 309.
- (33) Schwarz, R.; Gliemann, G.; Jolliet, P.; von Zelewsky, A. *Inorg. Chem.* **1989**, *28*, 742.
- (34) Maestri, M.; Sandrini, D.; Balzani, V.; von Zelewsky, A.; Jolliet, P. *Helv. Chim. Acta* **1988**, *71*, 134.
- (35) Craig, C. A.; Garces, F. O.; Watts, R. J. *Photochemistry and Photophysics of Coordination Compounds*; Yersin, H.; Vogler, A., Eds.; Springer Verlag: Berlin, **1987**; p 135.
- (36) Mäder, U.; Jenny, T.; von Zelewsky, A. *Helv. Chim. Acta* **1986**, *69*, 1085.
- (37) Zilian, A.; Mäder, U.; von Zelewsky, A.; Güdel, H. U. *J. Am. Chem. Soc.* **1989**, *111*, 3855.
- (38) Maestri, M.; Sandrini, D.; Balzani, V.; Mäder, U.; von Zelewsky, A. *Inorg. Chem.* **1987**, *26*, 1323.
- (39) Sandrini, D.; Maestri, M.; Balzani, V.; Mäder, U.; von Zelewsky, A. *Inorg. Chem.* **1988**, *27*, 2640.
- (40) Marcus, R. A. *J. Chem. Phys.* **1965**, *43*, 679.
- (41) Marcus, R. A. *J. Chem. Phys.* **1965**, *43*, 2654.
- (42) Sutin, N. *Accs. Chem. Res.* **1968**, *1*, 225.
- (43) Meyer, T. J. *Accs. Chem. Res.* **1978**, *11*, 94.
- (44) Lehn, J. M.; Ziessel, R. *Proc. Natl. Acad. Sci., U.S.A.* **1982**, *79*, 701.
- (45) Keene, F. R.; Creutz, C.; Sutin, N. *Coord. Chem. Rev.* **1985**, *64*, 247.
- (46) Katal, C.; Weber, M. A.; Ferraudi, G.; Geiger, D. *Organometallics* **1985**, *4*, 2161.
- (47) Katal, C.; Corbin, A. J.; Ferraudi, G. *Organometallics* **1987**, *6*, 553.
- (48) Hawecker, J.; Lehn, J. M.; Ziessel, R. *J. Chem. Soc., Chem. Commun.* **1983**, 536.
- (49) Halmann, M. *Energy Resources Through Photochemistry and Catalysis*; Grätzel, M., Ed., Academic Press: New York, **1983**.
- (50) Grant, J. L.; Goswami, K.; Spreer, L. O.; Otvos, J. W.; Calvin, M. J. *J. Chem. Soc., Dalton Trans.* **1987**, 2105.

photoreductions or they might be attached to electrode surfaces for use as catalysts in photoelectrochemical or electrochemical reductions. Readily formed dichloro-bridged dimers,^{55–61} such as $[\text{Ir}(\text{ppy})_2\text{Cl}]_2$, are solvated in strongly coordinating solvents (S) such as DMF, DMSO, and CH_3CN to yield solutions of mononuclear complexes, $[\text{Ir}(\text{ppy})_2\text{Cl}(\text{S})]$.⁶² However, attempts to isolate these have thus far failed due to re-formation of the original dichloro-bridged species.⁶³

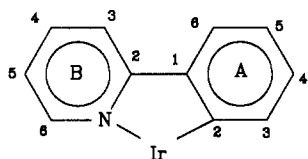
Quantitative removal of chloride from the dichloro-bridged compounds and subsequent isolation of solvated monometallic species can be achieved by treatment with soluble silver salts which remove chloride via AgCl precipitation. This approach has been used to prepare and isolate complexes of the type $[\text{Ir}(\text{L})_2(\text{S})_2][\text{OTf}]$ (L = 2-phenylpyridine (ppy) or 2-(*p*-tolyl)pyridine (ptpy); S = H_2O or CH_3CN ; OTf = CF_3SO_3^-).

Results

$[\text{Ir}(\text{L})_2(\text{H}_2\text{O})_2][\text{OTf}]$ (**2**). Silver trifluoromethanesulfonate (AgOTf) reacts with $[\text{Ir}(\text{L})_2\text{Cl}]_2$ (L = ppy (**1a**); L = ptpy (**1b**)) in a $\text{CH}_3\text{OH}/\text{CH}_2\text{Cl}_2$ solvent mixture (eq 1), giving $[\text{Ir}(\text{L})_2-$



$(\text{H}_2\text{O})_2][\text{OTf}]$ (**2a,b**). The ^1H NMR spectra of **2** in CDCl_3 show only seven (**2a**) or six (**2b**) signals in the aromatic region due to overlapping H3B and H4B resonances. Signals of the coordinated



H_2O are broad and do not integrate well, but the ^1H NMR spectrum of a concentrated solution of **2a** in CD_3OD shows eight well-resolved aromatic resonances and a singlet at 4.88 ppm which integrates 2:1 to the aromatic resonances. The latter signal is caused by the species CD_3OH , formed by proton/deuteron exchange between the CD_3OD and the H_2O ligands. The signals

- (51) DeLaet, D. L.; Fanwick, P. E.; Kubiak, C. P. *J. Chem. Soc., Chem. Commun.* **1987**, 1412.
 (52) Lemke, F. R.; DeLaet, D. L.; Gao, J.; Kubiak, C. P. *J. Am. Chem. Soc.* **1988**, *110*, 6904.
 (53) Belmore, K. A.; Vanderpool, R. A.; Tsai, J.-C.; Khan, M. A.; Nicholas, K. M. *J. Am. Chem. Soc.* **1988**, *110*, 2004.
 (54) Silavve, N. D.; Goldman, A. S.; Ritter, R.; Tyler, D. R. *Inorg. Chem.* **1989**, *28*, 1231.
 (55) Nonoyama, M. *Bull. Chem. Soc. Jpn.* **1974**, *47*, 767.
 (56) Nonoyama, M.; Yamasaki, K. *Inorg. Nucl. Chem. Lett.* **1971**, *7*, 943.
 (57) Hiraki, K.; Obayashi, Y.; Oki, Y. *Bull. Chem. Soc. Jpn.* **1979**, *52*, 1372.
 (58) Bruce, M. I.; Goodall, B. L.; Stone, F. G. A. *J. Organomet. Chem.* **1973**, *60*, 343.
 (59) Yin, C. C.; Deeming, A. J. *J. Chem. Soc., Dalton Trans.* **1975**, 2091.
 (60) Cockburn, B. N.; Howe, D. V.; Keating, T.; Johnson, B. F. G.; Lewis, J. *J. Chem. Soc., Dalton Trans.* **1973**, 404.
 (61) Kasahara, A. *Bull. Chem. Soc. Jpn.* **1968**, *41*, 1272.
 (62) Sprouse, S. D. *Electronic and Photophysical Properties of Substituted, Unsubstituted and Ortho-Metalated N-Heterocycle Complexes of Rh(III) and Ru(II)*. Ph.D. Dissertation, University of California, Santa Barbara, 1984.
 (63) Schmid, B. Unpublished results.
 (64) Garces, F. O.; Dedeian, K.; Keder, N. L.; Watts, R. J. *Acta Crystallogr.* in press.

Table 1. ^1H NMR Chemical Shifts^a and (Splitting Patterns)^b of Cyclometalated Ir(III) Complexes^c

proton position ^d	2a	3a	6a	2b	3b	6b
H3A	6.11 (d)	6.07 (d)	6.35 (d)	5.91 (s)	5.87 (s)	6.09 (s)
H4A	6.71 (t)	6.74 (t × d)	6.95 (t)			
H5A	6.87 (t)	6.88 (t × d)	7.08 (t) ^e	6.65 (d)	6.71 (d)	6.86 (d)
H6A	7.52 (d)	7.53 (d × d)	7.76 (d)	7.37 (d)	7.43 (d)	7.56 (d)
H3B	7.89 ^e	7.90 ^e	7.96 ^f	7.80 ^e	7.87 ^e	7.87 (d)
H4B	7.89 ^e	7.90 ^e	7.80 (t)	7.80 ^e	7.87 ^e	7.72 (t)
H5B	7.39 (m)	7.43 (m)	7.01 (m) ^e	7.28 (br)	7.37 (t)	6.94 (t)
H6B	9.02 (d)	9.08 (d)	7.52 (d)	8.92 (br)	9.04 (d)	7.36 (d)
CH ₃				2.03 (s)	2.04 (s)	2.14 (s)

^a δ , ppm, monitored in CDCl_3 solvent. ^b Splitting patterns of resonances are denoted as follows: (s) = singlet; (d) = doublet; (t) = triplet; (m) = multiplet; (br) = broad resonance; (d × d) = doublet of doublets; (t × d) = triplet of doublets. ^c **2a** = $[\text{Ir}(\text{ppy})_2(\text{H}_2\text{O})_2]^+$; **2b** = $[\text{Ir}(\text{ptpy})_2(\text{H}_2\text{O})_2]^+$; **3a** = $[\text{Ir}(\text{ppy})_2(\text{CH}_3\text{CN})_2]^+$; **3b** = $[\text{Ir}(\text{ptpy})_2(\text{CH}_3\text{CN})_2]^+$; **6a** = $[\text{Ir}(\text{ppy})_2(\text{bpy})]^+$; **6b** = $[\text{Ir}(\text{ptpy})_2(\text{bpy})]^+$. ^d For numbering of proton positions see diagram in text. ^e Overlapping resonances; chemical shift taken from the center of the signal. ^f Overlapped by a proton resonance of the bpy ligand.

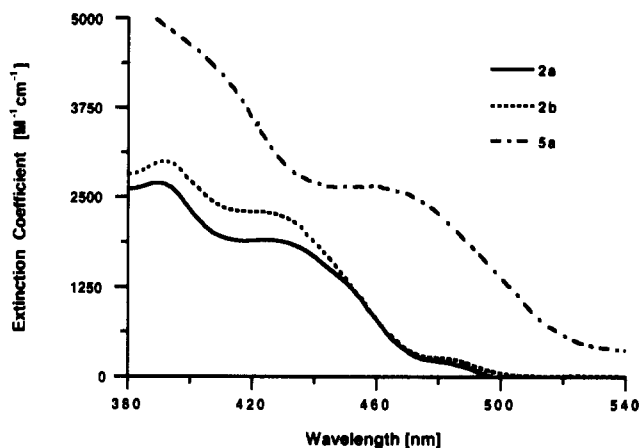


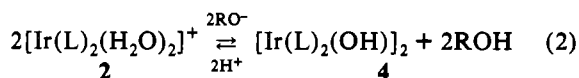
Figure 1. Absorption spectra of Bis(ortho-metalated) complexes of Ir(III) and Ir(IV): (---) $[\text{Ir}^{\text{III}}(\text{ppy})_2(\text{H}_2\text{O})_2][\text{OTf}]$ (**2a**) in dichloromethane; (---) $[\text{Ir}^{\text{III}}(\text{ptpy})_2(\text{H}_2\text{O})_2][\text{OTf}]$ (**2b**) in dichloromethane; (---) $[\text{Ir}^{\text{IV}}(\text{ppy})_2(\text{CH}_3\text{CN})_2][\text{OTf}]_2$ (**5a**) in acetonitrile.

in complexes **2** were assigned (Table 1) by analysis of their respective splitting patterns and by comparison with ^1H NMR spectra of **1**.⁶⁵

The ^{13}C NMR spectrum of **2a** shows 11 resonances in the aromatic region in agreement with the proposed composition of the complex. The signal at 138.7 ppm could be unambiguously assigned to the metalated C-atom, C2A, because of its weak intensity and its chemical shift. In the ^{13}C NMR spectrum of **2b** however, only 10 resonances are resolved in the aromatic region, rather than the anticipated 11 resonances, and this is probably due to overlapping signals.

The absorption spectra of **2** show similar features (Figure 1) in the UV-vis region. There is a fairly sharp band (390–392 nm) which overlaps a weaker band around 422–426 nm (Table 2). The extinction coefficient of a third band (480–484 nm) is only about $260 \text{ M}^{-1} \text{ cm}^{-1}$.

The reaction of $[\text{Ir}(\text{L})_2(\text{H}_2\text{O})_2][\text{OTf}]$ (**2a,b**) with 2 equiv of NaOR (R = Me or Et) in the corresponding alcohol leads to formation of the dinuclear compounds $[\text{Ir}(\text{L})_2(\text{OH})]_2 \cdot n \text{H}_2\text{O}$ (**4a,b**) according to eq 2. Compounds **4** are sparingly soluble



orange solids and therefore NMR spectra were limited by dynamic range considerations. However, the signal for the bridging OH

(65) Garces, F. O.; Watts, R. J. *Magn. Reson. Chem.*, in press.

Table 2. Absorption Data for $[\text{Ir}(\text{L})_2(\text{S})_2]^{n+}$ Complexes (2, 3, 5)

complex	abs features (nm)	extinction coeff (ϵ , $\text{M}^{-1} \text{cm}^{-1}$)
$[\text{Ir}(\text{ppy})_2(\text{H}_2\text{O})_2]^+ \text{ (2a)}$	480	286
	426 (sh)	1916
	390 (sh)	2824
$[\text{Ir}(\text{ptpy})_2(\text{H}_2\text{O})_2]^+ \text{ (2b)}$	484	248
	422 (sh)	2282
	392 (sh)	3080
$[\text{Ir}(\text{ppy})_2(\text{CH}_3\text{CN})_2]^{2+} \text{ (3a)}$	464	70
	395 (sh)	3500
	374	4590
$[\text{Ir}(\text{ptpy})_2(\text{CH}_3\text{CN})_2]^{2+} \text{ (3b)}$	470	110
	394 (sh)	4120
	374	4850
$[\text{Ir}(\text{ppy})_2(\text{CH}_3\text{CN})_2]^{2+} \text{ (5a)}$	465	2670
	400 (sh)	4500
	345 (sh)	7500

^a Monitored in CH_2Cl_2 solvent. ^b Monitored in butyronitrile solvent, CH_3CN ligands replaced by butyronitrile. ^c Monitored in CH_3CN solvent.

Table 3. ^{13}C NMR Chemical Shifts^a of $[\text{Ir}(\text{L})_2(\text{CH}_3\text{CN})_2]^{2+}$ (3)

carbon position ^b	$[\text{Ir}(\text{ppy})_2(\text{CH}_3\text{CN})_2]^+ \text{ (3a)}$	$[\text{Ir}(\text{ptpy})_2(\text{CH}_3\text{CN})_2]^+ \text{ (3b)}$
C2B	167.0	167.2
C3B	119.0	118.7
C4B	138.2	138.1
C5B	122.4	122.8
C6B	151.0	150.9
C1A	143.9	143.8
C2A	143.6	141.3
C3A	131.1	132.1
C4A	129.7	139.9
C5A	123.3	123.6
C6A	123.8	123.8
CH_3		21.5

^a δ , ppm, monitored in CDCl_3 solvent. ^b For numbering of carbon positions see diagram in text.

group in **4a** could be detected at 3.77 ppm.⁶⁶ The IR spectrum of **4a** (KBr pellet) shows a broad band at 3300 cm^{-1} indicating H_2O in the crystal lattice, and elemental analysis of **4a** is in best agreement with $n = 1/2$. The addition of HOTf to a slurry of **4a** in CD_3OD yields **2a** as monitored by ^1H NMR spectroscopy.

$[\text{Ir}(\text{L})_2(\text{CH}_3\text{CN})_2][\text{OTf}]$ (**3**). AgOTf reacts with $[\text{Ir}(\text{L})_2\text{Cl}]_2$ ($\text{L} = \text{ppy}, \text{ptpy}$) (**1a,b**) in acetonitrile (eq 1), giving $[\text{Ir}(\text{L})_2(\text{CH}_3\text{CN})_2][\text{OTf}]$ (**3a,b**). The ^1H NMR spectra of **3** in CDCl_3 (Table 1) show only seven (**3a**) or six (**3b**) aromatic signals due to overlapping H3B and H4B resonances; additional signals due to diethyl ether (from recrystallization), water, and CHCl_3 are seen, but no other signals due to possible impurities are observed. The signals were assigned by analysis of their splitting patterns and by comparison with $[\text{Ir}(\text{L})_2(\text{bpy})]^+$ (**6a,b**).⁶⁵ The two $\text{CH}_3\text{-CN}$ ligands give rise to a singlet at 2.35 ppm (**3a**) or 2.38 ppm (**3b**), respectively, which integrates 3:1 to the aromatic resonances. The ptpy-methyl resonance in **3b** appears as a singlet at 2.04 ppm.

The aromatic region of the ^{13}C NMR spectra of complexes **3** (Table 3) shows the 11 resonances expected for their proposed composition, with added signals at 118.9 ppm and at 3.8 ppm (due, respectively, to the CN and CH_3 carbon resonances of coordinated CH_3CN). The resonances of **3b** were assigned by application of heteronuclear COSY $^1\text{H}-^{13}\text{C}$ techniques, whereas those in **3a** were assigned by comparison with the ^{13}C resonance assignments of **3b**. The ^{13}C chemical shifts of corresponding C atoms in these two complexes are identical to within 1 ppm, except for those due to C4A and the metalated C2A carbon atoms.

Dissolution of **3a** in CD_3OD results in partial solvent exchange for CH_3CN as evidenced by the appearance of the signal for free

Table 4. Nuclear Overhauser Difference Spectral Results, $[\text{Ir}(\text{ptpy})_2(\text{CH}_3\text{CN})_2]^+ \text{ a}$

^1H resonance saturated (δ , ppm) ^b	% saturation	^1H resonance enhanced (δ , ppm) ^b	% enhancement
H6B (9.04)	63.1	H3B/H4B (7.87)	-1.0
		H5B (7.37)	6.7
		H3A (5.87)	2.6
H3A (5.87)	69.9	H6B (9.04)	2.3
		H5A (6.71)	-2.0
CH_3 (2.04)	63.3	CH_3 (2.04)	0.2
		H5A (6.71)	6.7
		H3A (5.87)	10.7

^a All measurements were performed on the complex dissolved in CD_3CN . ^b For numbering of proton positions see diagram in text.

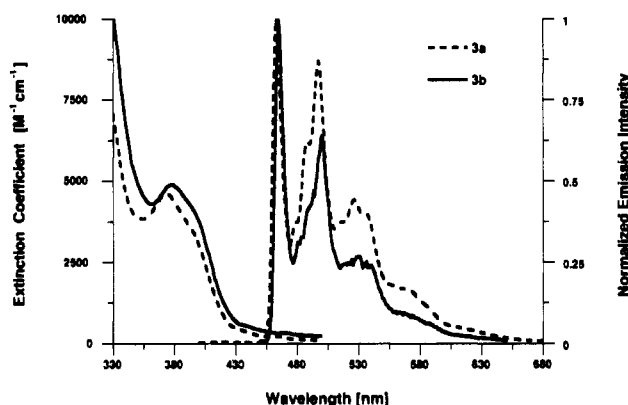


Figure 2. Absorption spectra at 298 K (left side) and emission spectra at 77 K (right side) of bis(ortho-metalated) butyronitrile complexes of Ir(III); (---) $[\text{Ir}(\text{ppy})_2(\text{PrCN})_2][\text{OTf}]$ (**3a**) in butyronitrile; (—) $[\text{Ir}(\text{ptpy})_2(\text{PrCN})_2][\text{OTf}]$ (**3b**) in butyronitrile.

CH_3CN in the ^1H NMR spectrum. Integration indicates nearly equal signals due to free and coordinated CH_3CN , suggesting that the primary species in these solutions is $[\text{Ir}(\text{ppy})_2(\text{CH}_3\text{CN})-(\text{CD}_3\text{OD})]^+$. As expected, the aromatic region of the spectrum in CD_3OD solutions is complicated due to the presence of unsymmetric species. The ^1H NMR spectrum of **3a** in reagent grade CDCl_3 also shows a signal for uncoordinated CH_3CN due to ligand exchange with residual H_2O in the deuterated solvent.

To further characterize the structure of **3b**, nuclear Overhauser enhancement difference spectroscopy was utilized. In these experiments, proton resonances at 9.04 ppm (H6B), 5.87 ppm (H3A) and 2.04 ppm (CH_3) were saturated; enhanced resonances are summarized in Table 4.

The emission spectra of **3** were recorded in butyronitrile (PrCN) solutions since this solvent is known to form clear glasses at 77 K. From evidence described above it is clear that CH_3CN is replaced by PrCN in this solvent; the species monitored under these conditions is $[\text{Ir}(\text{L})_2(\text{PrCN})_2]^+$. However, the similarity of CH_3CN and PrCN as ligands suggests that little difference is anticipated in the absorption and emission characteristics of the PrCN complex as compared to the CH_3CN complex. The absorption spectra of complexes **3** are very similar in the UV-vis region (Figure 2). Both show intense overlapping bands with maxima at 374 and 395 nm, although the extinction coefficients for **3b** are somewhat larger than those for **3a** (Table 2).

The emission spectra of **3** in 77 K butyronitrile glasses (Figure 2) consist of a progression of four bands with two sharp peaks and two weaker shoulders (Table 5). Additional, unresolved structure is also observed between 480 and 540 nm. Luminescence decays of both complexes are exponential with lifetimes of 7.7 μs (**3a**) and 9.3 μs (**3b**) (Table 5). Although these emissions are quite intense for samples at 77 K, no emission could be observed from PrCN solutions of the samples at room temperature.

Cyclic voltammetric analysis of complexes **3** consist of one reversible oxidation wave and one irreversible reduction wave for each complex (Table 5). The reduction of **3b** requires a more

(66) Read, M. C.; Glaser, J.; Sandström, M.; Toth, I. *Inorg. Chem.* **1992**, *31*, 4155.

Table 5. Cyclic Voltammetric^a and Emission^b Data and Estimated Excited State Reduction Potentials of $[\text{Ir}(\text{L})_2(\text{CH}_3\text{CN})_2]^+$ (3)

complex	emission features (nm)	τ^c (μs)	$E_{1/2}$ (V vs $\text{Fc}^{+/0}$)		ξ^o (V vs NHE) ^f	
			$E_{1/2}$ (ox)	$E_{1/2}$ (red)	ξ^o ($*1^+/0$) ^d	ξ^o ($2+/*1^+$) ^e
3a ^g	463, 497, 526, 565	7.7	0.88	-2.35 (irr)	1.01	-1.12
3b ^h	465, 500, 521, 565	9.3	0.90	-2.41 (irr)	0.94	-1.09

^a Cyclic voltammetric measurements were performed on argon-saturated CH_3CN solutions of the complexes at room temperature; 0.1 M tetrabutylammonium hexafluorophosphate was used as supporting electrolyte; potential of ferrocenium/ferrocene ($\text{Fc}^{+/0}$) reference versus SCE was 0.44 V. ^b Emission measurements were performed on argon-saturated butyronitrile glass solutions of the complexes at 77 K. ^c Emission lifetime. ^d Estimated standard potential for the couple $*[\text{Ir}(\text{L})_2(\text{CH}_3\text{CN})_2]^+ / [\text{Ir}(\text{L})_2(\text{CH}_3\text{CN})_2]^0$ where $*$ indicates the emissive excited state. ^e Estimated standard potential for the couple $[\text{Ir}(\text{L})_2(\text{CH}_3\text{CN})_2]^{2+} / *[\text{Ir}(\text{L})_2(\text{CH}_3\text{CN})_2]^{1+}$ where $*$ indicates the emissive excited state. ^f Converted from potential versus $\text{Fc}^{+/0}$ by adding 0.68 V. No corrections for changes in liquid junction potentials in different solvents are included in this conversion. ^g **3a** = $[\text{Ir}(\text{ppy})_2(\text{CH}_3\text{CN})_2]^+$. ^h **3b** = $[\text{Ir}(\text{ptpy})_2(\text{CH}_3\text{CN})_2]^+$.

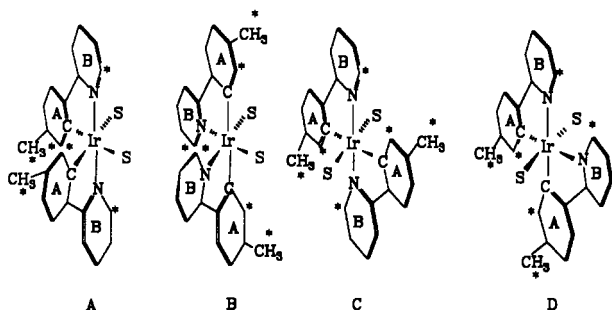


Figure 3. Schematic structural representations of geometric isomers of *cis*- and *trans*- $[\text{Ir}(\text{ptpy})_2(\text{CH}_3\text{CN})_2]^+$. Positions of protons whose resonances were saturated during nuclear Overhauser effect experiments are denoted with an asterisk.

cathodic potential than that of **3a**, whereas their oxidations occur at about the same potential. Electrochemical oxidation of **3a** in CH_3CN by controlled-potential coulometry yields the species, $[\text{Ir}(\text{ppy})_2(\text{CH}_3\text{CN})_2]^{2+}$ (**5a**). The UV-vis spectrum of a solution of **5a** (Figure 1) differs from the spectrum of **3a** primarily due to an added absorption band at 465 nm with an extinction coefficient of $2760 \text{ M}^{-1} \text{ cm}^{-1}$ (Table 2).

Discussion

Structure Determinations. The seven (ptpy complexes) or eight (ppy complexes) aromatic proton resonances seen in **2** and **3** indicate that each contains either a C_2 axis or a mirror plane. Structures which satisfy this requirement are illustrated as A-D in Figure 3. The crystal structure of the starting material **1b** used to prepare **2b** and **3b** contains Ir-C bonds located *trans* to the bridging chlorides,⁶⁴ and unless a geometric rearrangement occurs under the relatively mild conditions used to synthesize **2b** and **3b**, structural type A would be anticipated for these. Although crystals suitable for X-ray analysis could not be obtained for either **2** or **3**, ^1H NMR methods⁶⁵ provide strong evidence to confirm that **2a**, **2b**, **3a**, and **3b** are all described by structural type A.

The crystal structure of *trans*- $[\text{Ru}(\text{bpy})_2(\text{OH}_2)(\text{OH})]^{2+}$ establishes a maximum interatomic distance of 2.18(8) Å between the 6 and 6' protons of the *trans*-coordinated 2,2'-bipyridine ligands.⁶⁷ On the basis of these results, structural types C and D are regarded as unlikely possibilities. In the former case, the greatest nuclear Overhauser effect (nOe) would be expected

between the H6B and H3A resonances. In the latter case, no significant nOe relationship would be anticipated between the 9.04 ppm H6B proton resonance and the 5.87 ppm H3A proton resonance. The result of the nOe study (Table 4) falls between these two extremes as indicated by the 2.6% enhancement of resonance H3A and a 6.7% enhancement of the adjacent H5B resonance upon irradiation of the H6B signal. Controlled nOe studies of **1b** show that a maximum enhancement of 11.4% is achieved between the H5B and H6B protons which have an interatomic distance of 2.49 Å.⁶⁴

Although nOe difference spectroscopy is useful in showing structural types C and D to be unlikely for **2** and **3**, this method is less useful in distinguishing between structural types A and B. The H6B and H3A protons are located close to one another in both of these structural isomers, and similar nOe's are anticipated for each. However, assignment of the H3A proton to the highest field aromatic resonance and the H6B proton to the lowest field aromatic resonance is consistent with an NC ligand arrangement in which the H3A protons are highly shielded by interaction with an adjacent phenyl-ring and the H6B protons are relatively deshielded by an adjacent ligated CH_3CN ; this situation is realized in structural type A, but not in B. In structural isomer B the anticipated H6B resonance position can be estimated by considering prior ^1H NMR assignments^{11,68} of $[\text{Ir}(\text{bpy})_2(\text{bpy}-C^3, N')^{2+}]$ and $[(\text{Ir}(\text{bpy})(\text{bpy}-C^3, N')\text{Cl})_2]^{2+}$. In both of these species H6B is in a shielded environment, positioned over the π -cloud of an adjacent pyridyl ring. The resonances due to H6B are at 7.76 and 7.54 ppm, respectively, and a similar chemical shift would be anticipated for H6B in structural isomer B. The observed resonance at 9.04 ppm indicates a far less shielded environment for the H6B resonance than the one anticipated for the B isomer.

Finally, consider the chemical shift comparison of the proton adjacent to the metalated carbon atom in species **2** and **3** with the one in $[(\text{Ir}(\text{bpy})(\text{bpy}-C^3, N')\text{Cl})_2]^{2+}$ (H4A is bonded next to the metalated C atom in the numbering scheme used to label pyridyl ring positions in this complex). The resonance due to the H4A proton in this complex is found at 8.50 ppm due to its position in a relatively deshielded environment over the bridging chlorides.¹¹ If structural isomer B were indeed the configuration for complexes **2** and **3**, then the H3A resonance, like that of H4A in $[(\text{Ir}(\text{bpy})(\text{bpy}-C^3, N')\text{Cl})_2]^{2+}$, would be expected above ~ 8.0 ppm as opposed to its observed position at 5.87–6.11 ppm (Table 1). These factors taken together provide a compelling case for assignment of the structures of complexes **2** and **3** as isomers of the type represented by A.

Absorption and Emission Assignments. The strong absorption features ($\epsilon \sim 10^3$ – $10^4 \text{ M}^{-1} \text{ cm}^{-1}$) in the 350–410-nm region for both **2** and **3** (Table 2) are similar to those which have been reported in other monomeric bis(ortho-metalated) Ir(III) complexes.^{6,10} By analogy with prior assignments of bands in this region, these are attributed to spin-allowed MLCT transitions in which electron density is transferred from the Ir(III) to the π -system of the ortho-metalating ligands.

Complexes **2** and **3** display weaker absorption features at longer wavelengths. These appear at 460–470 nm ($\epsilon \sim 10^2 \text{ M}^{-1} \text{ cm}^{-1}$) for **3** while in **2** features at 480–490 nm ($\epsilon \sim (2\text{--}3) \times 10^2 \text{ M}^{-1} \text{ cm}^{-1}$) are partially resolved (Figure 2). Absorption bands similar in position to those in **3** have been reported¹⁰ for other bis(ortho-metalated) complexes, such as $[\text{Ir}(\text{L})_2(\text{bpy})]^+$ (**6**), although their extinction coefficients were 5–8 times greater than these. This is in a region where spin-forbidden bands due to both ligand-localized (LL) and MLCT states are anticipated, and prior studies indicate that extinction coefficients for these types of transitions range from about $10^1 \text{ M}^{-1} \text{ cm}^{-1}$ for those with mostly LL character to about $10^3 \text{ M}^{-1} \text{ cm}^{-1}$ for bands with mostly MLCT character.⁶⁹

(67) Durham, B.; Wilson, S. R.; Hodgson, D. J.; Meyer, T. J. *J. Am. Chem. Soc.* **1980**, *102*, 600.

(68) Spellane, P. J.; Watts, R. J.; Curtis, C. J. *Inorg. Chem.* **1983**, *22*, 4060.

(69) Watts, R. J.; Crosby, G. A. *J. Am. Chem. Soc.* **1972**, *94*, 2606.

Mixing of these two types is known to occur^{70,71} and the degree of mixing may be qualitatively related to the radiative lifetime under the assumption that the radiative decay rate of the LL state is negligibly small prior to mixing with a MLCT state. Under these circumstances, the radiative lifetime is determined by the fractional mixing of MLCT character into the LL configuration, and application of first order perturbation theory leads to the following result.⁷¹

$$1/\tau_0 = \{\beta/(E_{CT} - E_{LL})\}^2 \{E_{LL}^3/E_{CT}^3 \tau_0(CT)\} \quad (3)$$

In eq 3, τ_0 and $\tau_0(CT)$ represent the radiative lifetimes of the emitting excited state and the MLCT excited state which is mixed into the emitting state, respectively; β is the matrix element which mixes the LL and MLCT excited states, and; E_{CT} and E_{LL} are the energies of the MLCT and LL states, respectively. The Strickler-Berg equation,⁷² which adapts the earlier Einstein equation⁷³ for atomic transitions to those which occur in polyatomic species, provides a quantitative relationship between radiative lifetimes and the area under the integrated absorption band for an electronic transition. A simplified version of this equation which has been used for emitting triplet states is given by eq 4,⁷⁴ where K is a proportionality constant, E_T is the energy

$$1/\tau_0 = KE_T^2 \int \epsilon d\nu \quad (4)$$

of the emitting triplet state, and the integration is over the extinction coefficient versus frequency band area. Taking E_T in eq 4 to be given by E_{LL} in eq 3 gives eq 5. In a series of structurally

$$\int \epsilon d\nu = \{E_{LL}/KE_{CT}^3 \tau_0(CT)\} \{\beta/(E_{CT} - E_{LL})\}^2 \quad (5)$$

related species such as complexes 2 and 3, in which the primary charge transfer is from the Ir(III) metal center to the ortho-metalating ligands, the first term on the right of eq 5 is expected to be nearly constant. Therefore, the integrated absorption band area is roughly proportional to the quantity, $\{\beta/(E_{CT} - E_{LL})\}^2$, which is the square of the coefficient mixing the charge transfer configuration into the ligand localized configuration. The integrated absorption band is therefore a monitor of this mixing through eq 5 and a monitor of the anticipated radiative lifetime through eq 4.

Estimates of radiative lifetimes based upon eq 4 suggest that τ_0 values range from about 100 μ s for bands with $\epsilon_{max} \sim 10^4 \text{ M}^{-1} \text{ cm}^{-1}$ to about 1 μ s for $\epsilon_{max} \sim 10^3 \text{ M}^{-1} \text{ cm}^{-1}$. These estimates use band positions and shapes taken from those observed for complexes 2 and 3. As a result, the measured extinction coefficients ($(1-3) \times 10^2 \text{ M}^{-1} \text{ cm}^{-1}$) lead to radiative lifetime estimates of 3-10 μ s. The close correspondance of these estimates to the measured lifetime values for 3a and 3b (7.7 and 9.3 μ s, respectively) suggests that little shortening of the lifetime occurs due to radiationless deactivation in competition with radiative deactivation. Taking the low-energy absorption bands of complexes such as $[\text{Ir}(\text{ppy})_2(\text{bpy})]^+$ to be representative of transitions which are primarily MLCT in nature ($\epsilon \sim 10^3 \text{ M}^{-1} \text{ cm}^{-1}$), the extinction coefficients in complexes 2 and 3 are indicative of transitions to states which are best described as a strong admixture of both MLCT and LL character.

The absence of detectable room-temperature emission from complexes 3 contrasts the behavior of related Ir(III) complexes. For example, the intense emission of glass solutions of bischelated

bpy complexes,⁷⁵ such as $[\text{Ir}(\text{bpy})_2(\text{H}_2\text{O})_2]^{3+}$, at 77 K is only slightly quenched in ambient fluid solutions. Several sources for emission quenching of 3 in fluid solutions are possible. Non-radiative deactivation might result via either (a) thermal population of relatively low-energy metal-localized states which could be deactivated by both intramolecular conversion to the ground state and by photochemical ligand exchange between ligated and solvent CH_3CN , or (b) rapid intramolecular conversion and ligand exchange directly from the emissive MLCT excited state. The former mechanism was invoked to account for quenching of the emission and photochemical activity of $\text{Ru}(\text{bpy})_3^{2+}$ in fluid solutions⁷⁶⁻⁷⁹ and has since been used to account for similar behavior in a variety of metal complexes, including ortho-metalated Rh(III) complexes²⁶ such as $[\text{Rh}(\text{ppy})_2(\text{bpy})]^+$. The latter mechanism is considered because of the anticipated high energies of the metal-centered states of these Ir(III) complexes, which may render them thermally inaccessible, as well as the known tendency of these complexes to undergo ligand exchange reactions with coordinating solvents even in their ground states.

Rates for photochemical ligand exchange in metal centered excited states of d^6 complexes indicate that these can occur within a few hundreds of nanoseconds.^{80,81} While comparable results have not been established for ligand substitution in MLCT excited states of d^6 complexes, it is known that ligand dissociation occurs on the microsecond time scale from charge-transfer excited states of complexes of the type $(\text{Ph})_3\text{ERe}(\text{CO})_3\text{L}$ ($\text{E} = \text{Sn}$ or Ge ; $\text{L} = 1,10\text{-phenanthroline}$ or bpy).^{82,83} The excited states of these Re(I) complexes arise from transfer of Re-E bonding electrons to the bidentate ligand, and this is expected to have a greater impact upon ligand dissociation than does MLCT in a coordination complex. However, the well-known *trans*-labelizing effect of Ir-C bonds is probably responsible for the strong tendency of 3 to undergo thermal solvation reactions, and enhancement of the electron density on the metalating ligands via MLCT is likely to enhance these *trans*-labelizing effects. This might account for direct quenching of the emission via ligand exchange in these MLCT excited states.

The larger d-orbital splitting anticipated in Ir(III) ortho-metalated species in comparison with analogous Rh(III) complexes suggests that mechanism a, which has been proposed to account for quenching of cyclometalated Rh(III) complex emissions,²⁶ may not be equally applicable to the present Ir(III) species. Observation of relatively unquenched room-temperature emission in Ir(III) complexes⁷⁵ such as $[\text{Ir}(\text{bpy})_2(\text{H}_2\text{O})_2]^{3+}$ confirms that the metal-centered states of this complex are apparently too high in energy to bring about quenching and also indicates that this MLCT excited state does not participate directly in quenching via ligand exchange. Although the cyclometalated complex $[\text{Ir}(\text{ppy})_2(\text{bpy})]^+$ does emit at room temperature, the short lifetime in methanol (0.35 μ s) compared to the lifetime in 77 K glass (5.0 μ s), indicates substantial quenching in fluid solutions. The d-orbital splitting in this species is expected to be somewhat larger than that in $[\text{Ir}(\text{bpy})_2(\text{H}_2\text{O})_2]^{3+}$, so the quenching is unlikely to originate from thermal population of metal-centered

(70) DeArmond, M. K.; Hillis, J. E. *J. Chem. Phys.* **1971**, *54*, 2247.

(71) Watts, R. J.; Crosby, G. A.; Sansregret, J. L. *Inorg. Chem.* **1972**, *11*, 1474.

(72) Strickler, S. J.; Berg, R. *J. Chem. Phys.* **1962**, *37*, 814.

(73) Einstein, A. *Phys. Z.* **1917**, *18*, 121.

(74) Calvert, J. G.; Pitts, J. N. Jr. *Photochemistry*; Wiley: New York, 1962; p 191.

(75) Watts, R. J.; Harrington, J. S.; van Houten, J. *J. Am. Chem. Soc.* **1977**, *99*, 2179.

(76) Van Houten, J.; Watts, R. *J. Am. Chem. Soc.* **1975**, *97*, 3842.

(77) Van Houten, J.; Watts, R. *J. Am. Chem. Soc.* **1978**, *98*, 4853.

(78) Allsopp, S. R.; Cox, A.; Kemp, T. J.; Reed, W. *J. Chem. Soc., Faraday Trans. 1*, **1978**, *74*, 1275.

(79) Durham, B.; Casper, J. V.; Nagle, J. K.; Meyer, T. *J. Am. Chem. Soc.* **1982**, *104*, 4803.

(80) Bergkamp, M. A.; Brannon, J.; Magde, D.; Watts, R. J.; Ford, P. C. *J. Am. Chem. Soc.* **1979**, *101*, 4549.

(81) Bergkamp, M. A.; Watts, R. J.; Ford, P. C. *J. Am. Chem. Soc.* **1980**, *102*, 2627.

(82) Luong, J. C.; Faltynek, R. A.; Wrighton, M. S. *J. Am. Chem. Soc.* **1979**, *101*, 1597.

(83) Luong, J. C.; Faltynek, R. A.; Wrighton, M. S. *J. Am. Chem. Soc.* **1980**, *102*, 7892.

states. This suggests that quenching is largely a property of the MLCT excited state, as suggested by mechanism b, and may involve distortion of the Ir–N bonds of bpy by the *trans* effects due to the Ir–C bonds of ppy. Similar distortion of the Ir–N bond of coordinated CH₃CN by a *trans* effect of the Ir–C bond of ppy may lead to CH₃CN loss in the absence of the chelate effect which stabilizes [Ir(ppy)₂(bpy)]⁺ to bpy loss.

The estimated standard reduction potentials of complexes **3** in their excited states are included in Table 5. These estimates neglect entropy changes between the ground and excited states, and excited-state energies were taken from the position of the highest energy emission band in the luminescence spectrum at 77 K. Complexes **3** might be useful as both photooxidants and photoreductants although their use in homogeneous solutions is probably limited to electron-transfer reactions involving only a single electron. However, the ease with which CH₃CN can be removed indicates that they might readily be attached to electrode surfaces for possible use in electrocatalysis or photoelectrocatalysis of multiple electron oxidations and reductions. Means by which complexes **3** can be attached to electrode surfaces and used to promote multiple electron reduction of CO₂, particularly to methanol, are presently under investigation.

Experimental Section

Starting Materials and Solvents. [Ir(ppy)₂Cl]₂ and [Ir(ppy)₂Cl]₂ were prepared according to published procedures.^{10,56} Silver trifluoromethanesulfonate (AgOTf) and tetrabutylammonium hexafluorophosphate ((TBA)PF₆) were obtained from Aldrich and used without further purification. NaOR (R = methyl or ethyl) was prepared in situ by dissolving sodium in the corresponding alcohol. Solvents were reagent grade except for the UV grade acetonitrile used in cyclic voltammetry. All reactions were carried out under ambient conditions.

Instrumentation. ¹H NMR spectra were recorded at 300.13 MHz with a Nicolet NT-300 instrument or at 500.13 MHz with a General Electric GN-500 spectrometer. Chemical shifts were referenced to the residual proton signal of the deuterated solvents using the following values: δ = 7.26 ppm for chloroform, 3.30 ppm for methanol, and 2.05 ppm for acetone. ¹³C NMR spectra were recorded at 125.7 MHz with the GN-500 instrument. Chemical shift values were referenced to the signal of the deuterated solvent using δ = 77.0 ppm for chloroform and 49.0 ppm for methanol. Absorption spectra were measured with a Hewlett-Packard 8452A diode array spectrophotometer. Emission spectra were monitored with a Spex Fluorolog 2 spectrophotofluorimeter and were corrected for the instrumental response function to yield intensities proportional to the number of photons emitted. Luminescence decay curves were monitored and analyzed to yield lifetimes using a Laser Photonics UV-22 pulsed nitrogen laser for excitation. The optics, detection, and analysis apparatus used in these measurements has been described in a prior publication.⁸⁴ Cyclic voltammograms were measured with an IBM EC/225 voltammetric analyzer. Infrared spectra were monitored with a BIO-RAD FTS 60 instrument.

Preparation of Compounds. [Ir(ppy)₂(H₂O)₂][OTf] (**2a**). [Ir(ppy)₂Cl]₂ (53.6 mg, 50 μmol) was dissolved in 5 mL of methylene chloride and a solution of AgOTf (26.2 mg, 100 μmol) in 5 mL of methanol was added to yield a cream-colored slurry. After the slurry was stirred for 1 h, it was filtered through Celite and the filtrate was evaporated to dryness to yield a yellow, oily residue. This residue was dried under vacuum for 1 h to yield a hardened solid material. This material was collected and dried for an additional 16 h under vacuum to yield the product (65 mg, 95% yield). ¹³C NMR (125.7 MHz, methanol-*d*₄, ppm): δ 169.1 (C2B), 150.1 (C6B), 146.3 (C1A), 140.2 (C4B), 138.7 (C2A), 133.9, 130.5, 125.4, 124.0, 123.4, 120.4.

[Ir(ppy)₂(H₂O)₂][OTf] (**2b**). This was prepared and isolated in a manner analogous to **2a** above. ¹³C NMR (125.7 MHz, chloroform-*d*, ppm): δ 167.3 (C2B), 149.4 (C6B), 142.1 (C1A), 139.6 (C2A), 138.2*, 133.9, 123.7, 123.5, 121.9, 118.2, 21.5(CH₃) (asterisk denotes possibly two overlapping resonances).

[Ir(ppy)₂(OH)]₂·1/2H₂O (**4a**). [Ir(ppy)₂(H₂O)₂][OTf] (34.3 mg, 50 μmol) was dissolved in ROH (2 mL, R = CH₃ or CH₂CH₃). A solution of NaOR (50 μmol) in ROH (2 mL) was then added within 1 min, whereupon an orange precipitate gradually formed. The precipitate was collected on a filter and washed with alcohol, ether, and finally pentane and then dried under vacuum for 16 h to yield the product (22 mg, 84% yield). Anal. Calcd for C₄₄H₃₅N₄Ir₂O_{2.5}: C, 50.61; H, 3.38; N, 5.37. Found: C, 50.82; H, 3.64; N, 5.28. ¹H NMR (300.13 Mz, acetone-*d*₆, ppm): δ 9–6 (eight resonances), 3.77 (OH). Infrared (KBr, cm⁻¹): 1602 (m), 1581 (s), 1559 (m), 1544 (w), 1474 (s), 1438 (m), 1414 (s), 1301 (m), 1263 (m), 1224 (m), 1158 (m), 1068 (s), 1031 (m), 753 (s), 730 (s), 671 (w), 630 (w), 521 (w).

[Ir(ppy)₂(CH₃CN)₂][OTf] (**3a**). [Ir(ppy)₂Cl]₂ (194 mg, 0.181 mmol) and AgOTf (102 mg, 0.397 mmol) were placed in a flask. Acetonitrile (15 mL) was added, and the resulting slurry was stirred for 1 h. The solution was filtered through Celite and the precipitate was washed three times with CH₃CN (1-mL portions). The filtrate and washings were combined and reduced by evaporation to a volume of 1 mL. This solution was cooled to -10 °C, and ether (20 mL) was slowly added while stirring. The bright yellow precipitate which formed was collected by filtration and washed with ether and then pentane and dried under vacuum for 16 h to yield the product (224 mg, 85% yield).

[Ir(ppy)₂(CH₃CN)₂][OTf] (**3b**). This was prepared and isolated in a manner analogous to **3a** above in a yield of 70%.

[Ir(ppy)₂(CH₃CN)₂]²⁺ (**5a**). This was prepared by electrochemical oxidation of [Ir(ppy)₂(CH₃CN)₂][SbF₆] in CH₃CN solution. The electrolysis cell consisted of a cathode compartment composed of a Cu plate in contact with CuSO₄ (0.1 M) and an anode compartment composed of a Pt sheet in contact with a CH₃CN solution (25 mL, 0.1 M (TBA)PF₆ supporting electrolyte) of [Ir(ppy)₂(CH₃CN)₂][SbF₆] (6 mg, 7.3 μmol). A potential of 1.5 V was applied to the cell for 5 h to yield a dark yellow solution of the product in the anode compartment, which was characterized by UV-visible absorption spectroscopy.

Acknowledgment. The authors wish to thank G. A. Carlson for his assistance in measuring emission spectra. B.S. carried out this work during tenure of a fellowship from the National Energy Research Fund of Switzerland (NEFF). This work was supported by the Office of Basic Energy Sciences, United States Department of Energy, Contract DE-FG03-88ER13842.

(84) Wilde, A. P.; King, K. A.; Watts, R. J. *J. Phys. Chem.* **1991**, *95*, 629.